SIMS Proceedings Papers

SURFACE and INTERFACE ANALYSIS

Received: 30 September 2009 Revised: 15 February 2010 Accepted: 12 March 2010 Published online in Wiley Online Library: 11 May 2010

(wileyonlinelibrary.com) DOI 10.1002/sia.3417

Depth profiling by cluster projectiles as seen by computer simulations

Z. Postawa,[a]* L. Rzeznik,[a] R. Paruch,[a] M. F. Russo,[b] N. Winograd[b] and B. J. Garrison[b]

Molecular dynamics computer simulations are used to probe the development of the surface morphology and the processes that determine the depth resolution in depth profiling experiments performed by secondary ion and neutral mass spectrometry (SIMS/SNMS). The Ag(111) surface is irradiated by an impact of 20-keV Au_3, C_{60} and Ar_{872} clusters that represent a broad range of cluster projectiles used in SIMS/SNMS experiments. Improvements in the simulation protocol including automation and optimal sample shape allow for at least 1000 consecutive impacts for each set of initial conditions. This novel approach allows to shrink the gap between single-impact simulations and real experiments in which numerous impacts are used. **Copyright © 2010 John Wiley & Sons, Ltd.**

Keywords: molecular dynamics simulations; SIMS; cluster bombardment; depth profiling

Introduction

Bombardment of solids by energetic clusters has drawn significant attention since it has been experimentally found that a nonlinear or nonadditive enhancement of the sputtering or ejection yield occurs relative to bombardment by atomic projectiles.[1] Since then, numerous studies using both analytical approaches and computer modeling have been performed to investigate processes stimulated by cluster impacts.[2–4] In general, it has been found that the presence of the nonlinear yield enhancement is associated with the formation of a region of a high density of deposited energy. In this region, the assumption of binary collisions (linearity or one particle hitting another particle) is not fulfilled. This nonlinear behavior stimulated by energetic cluster bombardment has found numerous practical applications. One of the most important application is 3D chemical imaging of organic samples by SIMS.[5–11] In SIMS, the application of clusters such as SF_5, Au_3, Bi_3 and C_{60} which has been shown to stimulate a nonlinear enhancement of ion yield,[5,7] reduced chemical damage,[6] and reduced damage depth, has opened the door to a wide array of depth profiling capabilities, particularly of organic materials.[12–14]

Currently, the most popular cluster projectiles used in SIMS are Au_n/Bi_n ($n = 2,3$) and C_{60}. Recently, large noble gas clusters are being promoted into this field.[15–17] In the past several years there have been numerous computational studies that investigated the dynamics of sputtering by these projectiles.[4,18–34] However, almost all these studies were performed on a flat surface. In other words, the investigated impacts were independent and reflect the experimental condition of zero fluence. The results of computer simulations performed on flat surfaces are often related to experimental results, sometimes even those obtained at high fluence conditions. Surface topography does develop under high fluence conditions resulting in a surface that is far from flat,[35] therefore, it is relevant to verify to what extent such a comparison is justifiable. Performing simulations of high fluence experiments, however, is computationally challenging. There are numerous studies that investigate processes taking place at high fluence conditions for atomic projectiles by Monte Carlo (MC) approach.[36] However, MC technique cannot be applied to model impacts of cluster projectiles, as collective many-body interactions are the major driving force leading to particle ejection in this case.[21,22,25] Such processes cannot be modeled by MC due to binary collision approximation, which is a foundation of this approach. Molecular dynamics (MD) simulations are more general, but also much slower than MC. As a result, only a few MD attempts have been done to date to trace accumulated effects by multiple impacts of cluster projectiles.[30,33,34,37–39] Moseler *et al*. investigated the smoothing of thin film growth due to an energetic cluster impact on 'tilted' areas of the film.[37] Aoki *et al*. utilized a Si sample covered with artificially placed geometric blocks,[39] or a sample with predefined, sine wave, surface features[38] to examine the effects of the surface roughness on a smoothing process by Ar clusters of hundreds to thousands of atoms.

The current paper is a synthesis of recent modeling efforts used to characterize the development of the surface roughness during continuous irradiation of Ag(111) surface by 20-keV Au_3, C_{60} and Ar_{872} cluster projectiles and to probe the processes that determine the depth resolution in depth profiling experiments.

Model

Details of MD computer simulations used to model cluster bombardment are described elsewhere.[4,30] Briefly, the motion of the particles is determined by integrating Hamilton's equations

* *Correspondence to: Z. Postawa, Smoluchowski Institute of Physics, Jagiellonian University, ul. Reymonta 4, 30-059 Kraków, Poland. E-mail: zbigniew.postawa@uj.edu.pl*

a *Smoluchowski Institute of Physics, Jagiellonian University, ul. Reymonta 4, 30-059 Kraków, Poland*

b *Department of Chemistry, The Pennsylvania State University, University Park, PA 16802, USA*

Copyright © 2010 John Wiley & Sons, Ltd.

of motion. A 'divide and conquer' scheme for performing several impacts simultaneously, while preserving the time dependence of the impact sequence, developed by Russo *et al*. is applied to model sample evolution induced by continuous cluster irradiation.[30] The main sample used in this investigation consists of Ag(111) crystal measuring 53 × 53 × 27 nm. However, smaller local samples were extracted and used to calculate the system evolution for a single impact.[30] The sample used to simulate Au_3 impacts at normal incidence was cylindrical in shape with a radius of 8 nm and a height of 17 nm measured from the bottom of the deepest valley present in the local sample. All other impacts were calculated on samples that were a combination of a cylinder with a radius of 9 nm for C_{60} and 11 nm for Ar_{872} and a height of 10 nm measured from the bottom of the deepest valley, capped at the bottom with a hemisphere of the same radius. The shape and size of the samples were chosen based on visual observations of the shape and size of collision cascades stimulated by impacts of 20-keV Au_3, C_{60} and Ar_{872} projectiles on Ag(111), respectively. Rigid and stochastic regions measuring 0.7 and 2.0 nm, respectively, were used on the bottom as well as cylindrically around the sides to simulate the thermal bath that keeps the sample at required temperature, to prevent pressure waves, and to maintain the shape of the sample.[4,20] These outer layers also act as a sleeve that allows for the reinsertion of the modified coordinates back into the main sample without causing particles to overlap at the edges.

A molecular dynamics/Monte Carlo-corrected effective medium (MD/MC-CEM) potential was used to describe the Ag–Ag interactions during C_{60} bombardment.[40] However, as this potential has known problems when describing interactions in metal alloys,[4] the embedded atom potential (EAM) was used to represent Ag–Ag, Ag–Au and Au–Au interactions during Au_3 impacts.[41] The interaction between C atoms in the projectile were described by the adaptive intermolecular potential, AIREBO.[42] The interaction between Ar atoms as well as interactions between Ar and Ag atoms was described by a Lennard-Jones potential splined with KrC potential to properly describe high energy collisions.[43] The same potential with different parameters was used to describe interactions between C and Ag atoms.[21] Each individual impact was followed for 25, 20 and 30 ps for Au_3, C_{60} and Ar_{872}, respectively. Projectiles were directed onto each sample at 0 and 70° with respect to the normal to the original surface. A total of 850 impacts were performed per $(53\ nm)^2$ which corresponds to a fluence of $\sim 3.1 \times 10^{13}$ impacts/cm^2. The simulations were run at 0K target temperature to minimize the effect of the thermal processes (diffusion, segregation, etc.). As a result, mostly collision-induced phenomena are probed which makes the data easier for interpretation. However, the consequence of such approach is that the results can be directly compared only with the experimental data obtained at liquid nitrogen LN_2 or lower temperature.

Results and Discussion

Typical craters created by an impact of 20-keV Au_3, C_{60} and Ar_{872} projectiles at a flat surface are shown in Fig. 1 for normal impact. The presented craters were formed by impacts that result in a sputtering yield close to the average value. It is evident that the shape and size of the craters depend on the type of the projectile. The crater formed by an impact of the Au_3 cluster is elongated in the vertical direction with a relatively small opening. Although, the crater extends deep into the sample, a large fraction of the primary kinetic energy is deposited below the crater depth and cannot contribute to sputtering. While not contributing to ejection, this energy leads to a significant interlayer mixing as it was observed for atomic projectile.[21] The crater formed by C_{60} has a larger opening diameter and is shallower than the corresponding crater formed by Au_3 impact. The crater is also more azimuthally isotropic. The most laterally extended, but also the shallowest crater, is formed by Ar_{872} projectile. It is also important to note that the crystal volume altered by projectile impact is limited to a thin zone located in the vicinity of the crater walls for C_{60} and Ar_{872}. As a result, for these clusters, projectile-induced damage is well localized.

The difference in shapes of the craters formed by Au_3 and C_{60} or Ar_{872} projectiles is a consequence of different initial conditions of the penetrating clusters. As the gold atoms have a high kinetic energy (6666 eV/atom) and are heavier than the silver atoms, some of them travel deep into the sample creating disruption over a significant depth. For instance, for the trajectory shown in Fig. 1, the crater extends up to 3.5 nm, while the three Au atoms are implanted at a depth of 2.3, 6.7 and 16.3 nm, respectively. One consequence of such behavior has already been mentioned; that is, an elongated shape of the crater and a lower sputtering yield as compared to corresponding C_{60} or Ar_{872} impacts. Another consequence is a much larger effect of the increasing impact angle observed for the Au_3 projectile as compared to the medium-size or large clusters.[33] On the other hand, due to their large size, C_{60} and Ar_{872} projectiles interact strongly with the sample atoms.

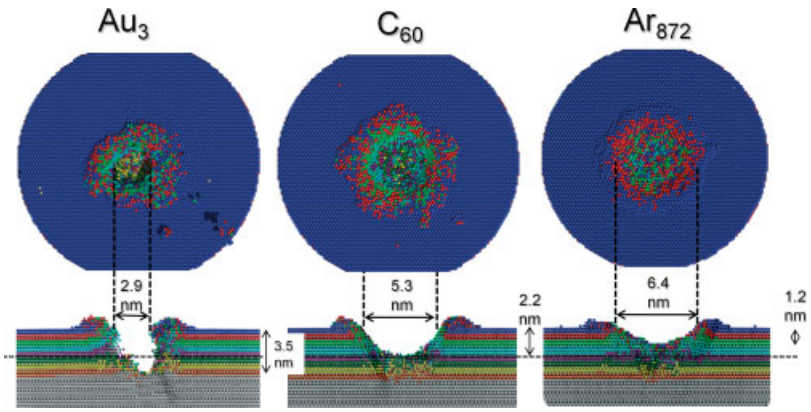

Figure 1. Top and cross-sectional side views of typical craters created by impact of 20 keV-Au_3, C_{60} and Ar_{872} at normal incidence at a flat Ag(111) surface at time of 30 ps. Color scheme depicts original location of atoms in a given layer. The cross-sectional view is 1.5 nm wide and is centered along the projectile impact point.

 Copyright © 2010 John Wiley & Sons, Ltd.

The process is almost mesoscopic in that the interaction of a projectile with the rest of the system is a many-body collision in which several projectile atoms simultaneously hit the same target atom.[19,21,25] The individual atoms in the cluster are not initiating their own collision cascades, rather, they are working cooperatively to move the target atoms. One of the consequences of such activity is generation of pressure waves that propagate in the sample.[19,20] After impact of the C_{60} and particularly Ar_{872} projectile on the Ag surface, the spatial correlation of the movements of atoms constituting the projectile is lost almost immediately. Consequently, the energy of the cluster projectile is deposited in a shallow volume of the sample in a short time, leading to the ejection of many particles. As a result, a large but relatively shallow and azimuthally isotropic crater is formed. The energy dependence studies show that the size of the crater, and consequently, the total sputtering yield increases with an increase of the initial kinetic energy.[21,22] The diameter of the crater is predominantly affected while its depth is less influenced.[21] It has been also reported that above certain energy threshold the dependence between total sputtering yield and the kinetic energy is linear.[9,22]

Owing to the heavier mass of the Ag atoms, most of the C or Ar atoms originating from the projectile are reflected towards the vacuum. We see that on average five carbon atoms are implanted in the Ag sample per single 20-keV C_{60} impact at normal incidence. This implantation occurs even though the interaction between the Ag and C atoms is very weak. It is interesting to note that under similar conditions, almost no Ar atoms get implanted. Even these few Ar atoms which find themselves below the surface effuse into the vacuum due to very low penetration depth caused by a low kinetic energy of the individual Ar atoms, and extremely weak interaction between inert Ar and Ag. Efficiency of deposition of projectile atoms depends on the chemical properties of both the sample and the projectile. Deposition of low-energy inert Ar atoms should remain minimal for all samples. As a result, the modification of the chemical structure will be small. It has been reported, however, that deposition of carbon atoms from C_{60} projectile at semiconductor surfaces can be severe.[28,44]

All predictions made so far have been derived from single impacts on a flat surface. The development of the surface morphology results in sputtering scenarios that are not present during flat surface bombardment.[30] Therefore, it is important to inquire as to what extent these predictions remain valid if measurements are performed on altered surfaces. The answer to this question depends on the type of information that one would like to extract. For instance, the sputtering yield for all three clusters studied here, irradiating Ag(111) surface at not too large impact angles, does not depend on the fluence, except for a small region at a low fluence ($<\sim 1 \times 10^{13}$ impacts/cm^2)[33] where the yield decreases. The shape of the kinetic energy distributions is also insensitive to the development of surface morphology.[33] On the other hand, the yield increases significantly with a fluence for medium and large cluster projectiles if the surface is irradiated at oblique impact angle.[33,45] The shape of the angular spectrum of ejected particles is also very sensitive to surface topography.[33] The quantitative estimates of the depth resolution that could be deduced from the data shown in Fig. 1 are also incorrect. Taking into account crater depth and the extent of the altered zone, one would estimate a depth resolution of ~3 nm for 20-keV C_{60} projectiles at normal incidence. The corresponding experimental value obtained in depth profiling studies of multilayer Cr–Ni samples is larger (~5–6 nm) for 20-keV C_{60} at 45° impact angle.[46]

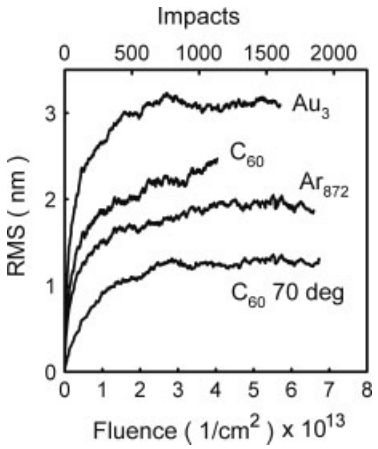

Figure 2. Root-mean-square roughness (in nanometers) of the entire sample versus the number of projectile impacts and the ion beam fluence for 20-keV Au_3, C_{60} and Ar_{872} at normal incidence, and 20-keV C_{60} at 70° impact angle.

To trace quantitatively the evolution of the surface morphology, the dependence of the root-mean-square (RMS) roughness of the investigated system on the projectile fluence is calculated and shown in Fig. 2. Two trends can be identified in the development of surface roughness. First, at the beginning, the value of the RMS increases fast. This fast increase terminates around 1×10^{13} impacts/cm^3 and is followed by a slow increase that finally goes into saturation. It is interesting to note that a decrease of the sputtering yield mentioned in the previous paragraph terminates roughly at the same fluence, which indicates that development of the surface topography have some influence on the sputtering yield. We attribute the initial fast increase to the fact that the roughness of the sample is rapidly changing due to the (artificially) flat surface starting conditions. This phase then moves into the more natural, slow decay caused by multiple bombardments. As expected from Fig. 1, the largest RMS is achieved by 20-keV Au_3 projectiles at normal incidence, while irradiation by Ar_{872} projectiles leads to formation of the least corrugated surface. The increase of the impact angle has a positive influence on the roughness leading to a less corrugated surface for off-normal bombardment. However, the effect becomes significant only for large oblique impact angles.[47] Studies on the effect of the primary kinetic energy and the impact angle on the surface roughness and the shape of the delta-layer depth profiles show that there is a direct correspondence between the final surface roughness, or RMS at saturation, and the ultimate depth resolution that one can achieve.[45,47] A similar conclusion was derived from experimental measurements performed at the organic delta-layers sputtered by C cluster ions.[9] This observation supports the preposition that the continuous increase of the depth resolution observed in some experiments is caused by experimental artifacts.[48] Finally, the computer generated images show that for projectiles with small penetration depth (for keV medium and large clusters), it is impossible to separate atomic relocations due to development of surface roughness from relocations caused by projectile-induced mixing. These studies also show that there is considerable lateral motion during bombardment. As a result, the average lateral displacement is much larger than the vertical relocation, and the most of relocated atoms are localized in the hills.[45]

View this article online at wileyonlinelibrary.com Copyright © 2010 John Wiley & Sons, Ltd.

SURFACE and INTERFACE ANALYSIS

Conclusions

We have examined the effect of the continuous irradiation by 20-keV Au_3, C_{60} and Ar_{872} projectiles on the development of surface topography, and the depth resolution in depth profiling experiments. There are several predictions that result from our studies. First, the surface roughness increases with the fluence reaching the saturation above a certain fluence or sputter depth. As the projectile-induced mixing is also limited to the penetration depth of the ion beam, which for a given primary kinetic energy is constant, these two observations indicate that the depth resolution should be constant after a certain fluence or sputter depth. This observation supports the preposition that the continuous increase of the depth resolution observed in some experiments is caused by experimental artifacts. Second, the rougher surface is formed during Au_3 impacts, while the smoother surface is achieved during Ar_{872} irradiation. A decrease of the primary kinetic energy and the increase of the impact angle have a positive influence on the surface roughness. The effect of the impact angle becomes significant only at oblique impact angles. We observe a direct relation between the RMS values at saturation and the depth resolution obtained from analysis of a delta layer profile. Finally, the effects caused by projectile-induced mixing and a development of the surface roughness are entangled and should not been separated, at least for medium and large cluster projectiles.

Acknowledgments

The authors would like to thank the Polish Ministry of Science and Higher Education Programs Nos PB 4097/H03/2007/33 and PB 0935/B/H03/2008/35, and the Chemistry Division of the National Science Foundation Grant Nos CHE-0910564 and Nos CHE-0908226, as well as the Department of Energy Grant No. DE-FG02-06ER15803, for their financial support of this research. The authors would also like to thank the Pennsylvania State University High Performance Computing Group for use of their computing resources and technical support.

References

[1] D. A. Thompson, S. S. Johar, *Appl. Phys. Lett.* **1979**, *34*, 342.
[2] H. H. Andersen, *VIDENSK SELSK MAT FY* **1993**, *43*, 127.
[3] H. M. Urbassek, in *Sputtering by Particle Bombardment, Vol. 110*, Springer-Verlag, Berlin, **2007**, pp 189.
[4] B. J. Garrison, Z. Postawa, *Mass Spectrom. Rev.* **2008**, *27*, 289.
[5] E. R. Fuoco, G. Gillen, M. B. J. Wijesundara, W. E. Wallace, L. Hanley, *J. Phys. Chem. B* **2001**, *105*, 3950.
[6] G. Gillen, L. King, B. Freibaum, R. Lareau, J. Bennett, F. Chmara, *J. Vac. Sci. Technol., A, -Vacuum Surfaces and Films* **2001**, *19*, 568.
[7] D. Weibel, S. Wong, N. Lockyer, P. Blenkinsopp, R. Hill, J. C. Vickerman, *Anal. Chem.* **2003**, *75*, 1754.
[8] A. Wucher, J. Cheng, N. Winograd, *Anal. Chem.* **2007**, *79*, 5529.
[9] A. G. Shard, F. M. Green, P. J. Brewer, M. P. Seah, I. S. Gilmore, *J. Phys. Chem. B* **2008**, *112*, 2596.
[10] E. A. Jones, N. P. Lockyer, J. C. Vickerman, *Anal. Chem*, **2008**, *80*, 2125.
[11] A. Wucher, J. Cheng, L. Zheng, N. Winograd, *Anal. Bioanal. Chem.* **2009**, *393*, 1835.
[12] N. Winograd, *Anal. Chem.* **2005**, *77*, 142A.
[13] A. Wucher, *Appl. Surf. Sci.* **2006**, *252*, 6482.
[14] C. M. Mahoney, *Mass Spectrom. Rev.* **2009**, DOI: 10.1002/mas.20233.
[15] S. Ninomiya, Y. Nakata, Y. Honda, K. Ichiki, T. Seki, T. Aoki, J. Matsuo, *Appl. Surf. Sci.* **2008**, *255*, 1588.
[16] K. Mochiji, M. Hashinokuchi, K. Moritani, N. Toyoda, *Rapid Commun. Mass Spectrom.* **2009**, *23*, 648.
[17] J. Matsuo, (*these proceedings, submitted*).
[18] R. Smith, R. P. Webb, *Proceedings of the Royal Society of London Series A-Mathematical Physical and Engineering Sciences* **1993**, *441*, 495.
[19] T. Seki, T. Aoki, M. Tanomura, J. Matsuo, I. Yamada, *Mater. Chem. Phys.* **1998**, *54*, 143.
[20] Z. Postawa, B. Czerwinski, M. Szewczyk, E. J. Smiley, N. Winograd, B. J. Garrison, *Anal. Chem.* **2003**, *75*, 4402.
[21] Z. Postawa, B. Czerwinski, M. Szewczyk, E. J. Smiley, N. Winograd, B. J. Garrison, *J. Phys. Chem. B* **2004**, *108*, 7831.
[22] C. Anders, H. M. Urbassek, *Phys. Rev. B* **2004**, *70*, 155404.
[23] A. Delcorte, *PCCP* **2005**, *7*, 3395.
[24] C. Szakal, J. Kozole, M. F. Russo Jr, B. J. Garrison, N. Winograd, *Phys. Rev. Lett.* **2006**, *96*, 216104.
[25] S. Zimmermann, H. M. Urbassek, *Nuclear Instruments and Methods in Physics Research Section B: Beam Interactions with Materials and Atoms* **2007**, *255*, 208.
[26] J. Samela, K. Nordlund, *Phys. Rev. B* **2007**, *76*, 125434.
[27] L. Rzeznik, B. Czerwinski, N. Winograd, B. J. Garrison, Z. Postawa, *J. Phys. Chem. C* **2008**, *112*, 521.
[28] K. D. Krantzman, B. J. Garrison, *J. Phys. Chem. C* **2009**, *113*, 3239.
[29] L. Rzeznik, B. Czerwinski, R. Paruch, B. J. Garrison, Z. Postawa, *Nuclear Instruments & Methods in Physics Research Section B-Beam Interactions with Materials and Atoms* **2009**, 1436.
[30] M. F. Russo, Z. Postawa, B. J. Garrison, *J. Phys. Chem. C* **2009**, *113*, 3270.
[31] R. Paruch, L. Rzeznik, B. Czerwinski, B. J. Garrison, N. Winograd, Z. Postawa, *J. Phys. Chem. C* **2009**, *113*, 5641.
[32] A. Delcorte, B. J. Garrison, K. Hamraoui, *Anal. Chem.* **2009**, *81*, 6676.
[33] R. Paruch, L. Rzeznik, M. F. Russo, B. J. Garrison, Z. Postawa, *J. Phys. Chem. C* **2010**, *114*, 5532.
[34] K. D. Krantzman, A. Wucher, *J. Phys. Chem. C* **2010**, *114*, 5480.
[35] W. O. Hofer, *Top. Appl. Phys.* **1991**, *64*, 15.
[36] H. Gnaser, *Low-energy ion irradiation of solid surfaces,* vol. 146, Springer. Berlin/Heidelberg, **1999**, p. 1.
[37] M. Moseler, O. Rattunde, J. Nordiek, H. Haberland, *Nuclear Instruments & Methods in Physics Research Section B-Beam Interactions with Materials and Atoms* **2000**, *164*, 522.
[38] T. Aoki, J. Matsuo, I. Yamada, *I. Mater. Res. Soc. Symp. Proc.* **2004**, 792.
[39] T. Aoki, J. Matsuo, *Nuclear Instruments and Methods in Physics Research Section B: Beam Interactions with Materials and Atoms* **2007**, *255*, 265.
[40] C. L. Kelchner, D. M. Halstead, L. S. Perkins, N. M. Wallace, A. E. Depristo, *Surf. Sci.* **1994**, *310*, 425.
[41] S. M. Foiles, M. I. Baskes, M. S. Daw, *Phys. Rev. B* **1986**, *33*, 7983.
[42] S. J. Stuart, A. B. Tutein, J. A. Harrison, *J. Chem. Phys.* **2000**, *112*, 6472.
[43] R. A. Aziz, M. J. Slaman, *Mol. Phys.* **1986**, *58*, 679.
[44] G. Gillen, J. Batteras, C. Michaels, P. Chi, J. Small, E. Windsor, A. Fahey, J. Verkouteren, K. J. Kim, *Appl. Surf. Sci.* **2006**, *252*, 6521.
[45] L. Rzeznik, R. Paruch, M. F. Russo, B. J. Garrison, Z. Postawa, *J. Phys. Chem. C*, (*in preparation*).
[46] S. Sun, A. Wucher, C. Szakal, N. Winograd, *Appl. Phys. Lett.* **2004**, *84*, 5177.
[47] R. Paruch, L. Rzeznik, B. J. Garrison, Z. Postawa, *Anal. Chem.*, (*in preparation*).
[48] L. Zheng, A. Wucher, N. Winograd, *Anal. Chem.* **2008**, *80*, 7363.

 Copyright © 2010 John Wiley & Sons, Ltd. View this article online at wileyonlinelibrary.com